

Quantum Impurity Models coupled to Markovian and Non Markovian Baths

Orazio Scarlatella¹ and Marco Schiro¹

Institut de Physique Théorique, Université Paris Saclay, CNRS, CEA, F-91191 Gif-sur-Yvette, France

(Dated: 23 November 2021)

We develop a method to study quantum impurity models, small interacting quantum systems linearly coupled to an environment, in presence of an additional Markovian quantum bath, with a generic non-linear coupling to the impurity. We aim at computing the evolution operator of the reduced density matrix of the impurity, obtained after tracing out all the environmental degrees of freedom. First, we derive an exact real-time hybridization expansion for this quantity, which generalizes the result obtained in absence of the additional Markovian dissipation, and which could be amenable to stochastic sampling through diagrammatic Monte Carlo. Then, we obtain a Dyson equation for this quantity and we evaluate its self-energy with a resummation technique known as the Non-Crossing-Approximation. We apply this novel approach to a simple fermionic impurity coupled to a zero temperature fermionic bath and in presence of Markovian pump, losses and dephasing.

I. INTRODUCTION

Small interacting quantum systems coupled to external environments represent basic paradigms of transport, dissipation and non equilibrium phenomena. Understanding the dynamical behavior of these open quantum systems is therefore crucial in many different physical contexts where the idealization of an isolated quantum system obeying perfectly unitary quantum dynamics is either too restrictive or unable to capture the fundamental physics.

In condensed matter physics the motivation comes from studying models of quantum dissipation and macroscopic quantum tunneling in the early days of Caldeira-Leggett and spin-boson models^{1,2} which keep attracting a lot of interest³ or from diluted magnetic impurities in metals⁴ and transport through quantum dots and single molecules attached to leads^{5–8} leading to fermionic realizations of so called quantum impurity models. These consist of a small quantum systems with few interacting degrees of freedom, the impurity, coupled via hybridization to a gapless reservoir of fermionic or bosonic excitations. The dynamical correlations of such reservoirs, which decay in time as a power law at zero temperature and feature strong memory effects⁹, together with a local many body interaction, make quantum impurity physics highly non trivial. Nevertheless, methods to solve the dynamics of quantum impurity models have flourished in recent years, mainly driven by the developments of Diagrammatic Monte Carlo^{10–18}.

On a different front, recent advances in quantum optics, quantum electronics and quantum information science have brought forth novel classes of driven open quantum systems in which excitations are characterized by finite lifetime due to unavoidable losses, dephasing and decoherence processes originating from their coupling to an external electromagnetic environment. Examples include atomic and optical systems such as ultracold gases in optical lattices¹⁹ or trapped ions²⁰, as well as solid state systems such as arrays of nonlinear superconducting microwave cavities^{21,22}. In these settings,

the dissipative processes associated to the external environment can be very well described in terms of a Lindblad master equation for the system density matrix²³. A major effort here is to conceive situations in which coupling to a quantum environment can involve non-linear combinations of system operators thus mediating effective interactions which act as a resource for quantum state preparation and to engineer a desired steady state. Such a dissipation engineering is actively investigated in quantum optics^{24–26}. This has stimulated a new wave of interest around open Markovian quantum systems at the interface between quantum optics and condensed matter physics.

The examples above represent two well studied, yet substantially separated, paradigms of open quantum systems. At the same time much less is known about the interface between those two settings, namely the interplay between Markovian dissipation and the coupling to a fully structured, frequency dependent, Non-Markovian quantum bath. Such a question is potentially relevant in a number of contexts. From one side, mesoscopic quantum devices have been successfully coupled to electromagnetic resonators hosting dissipative photon fields^{27–30} offering the possibility to investigate the fate exotic many body phases such as the Kondo effect in presence of Markovian dissipation. On the other hand, in the context of quantum optics and quantum information the role of Non-Markovian bath correlations has been recently attracting enormous interest^{31–33} and there is urgent need to develop novel theoretical approaches to address this question.

With these motivations, in this work we focus on a model for a quantum impurity coupled to two kind of external environments, as depicted in figure 1: a quantum bath described by a set of non interacting modes linearly coupled to our impurity degree of freedom, as in conventional quantum impurity models, resulting in a frequency dependent Non-Markovian evolution for the impurity and a second environment, where the non interacting bath modes can be also non-linearly coupled to the impurity, but for which the reduced impurity dy-

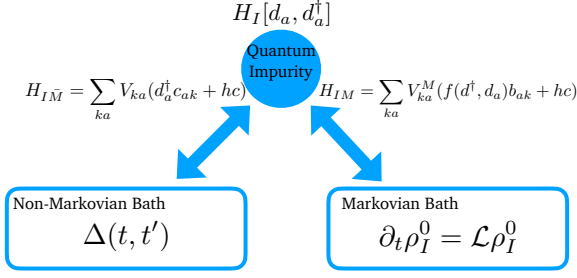


FIG. 1. Schematic plot of the setup considered in this manuscript. A small quantum system (impurity) is (i) linearly coupled to a quantum bath whose non trivial correlations, encoded in the hybridization function $\Delta(t, t')$, lead to Non-Markovian behavior and (ii) coupled non-linearly to a Markovian bath whose effect on the impurity is described by a Lindblad master equation. The resulting quantum impurity model with mixed Markovian and Non-Markovian dissipation is studied using hybridization expansion techniques.

namics would be well described by a Markovian master equation. The resulting impurity problem encodes therefore the interplay between those two kind of dissipative mechanisms and the local interaction on the impurity.

Taking inspiration from recent developments in quantum impurity physics we develop here an hybridization expansion for the real-time evolution operator of the impurity, obtained after tracing out both the non-Markovian environment, as usually done in the literature, as well as the Markovian bath. The final result naturally generalizes the well known real-time hybridization expansions to this mixed Markovian/Non-Markovian context. In addition to its own interest and potential for the development of diagrammatic Monte Carlo sampling, this expansion allows us to formulate a self-consistent resummation technique for the real-time impurity evolution operator based on the Non-Crossing-Approximation used in the context of quantum impurity models. We derive and discuss in details this approach and test it on a simple fermionic model coupled to a zero temperature bath and in presence of Markovian dissipation.

The paper is organized as follows. In Section II we introduce the model and the general formulation of the problem. Section III is devoted to derive the hybridization expansion for the real-time impurity propagator, after tracing out the non-Markovian bath (section III.A) and the Markovian environment (Section III.B). In Section IV we develop a self-consistent resummation based on the Non Crossing Approximation while in Section V we apply this method to a simple model.

II. MODEL AND GENERAL FORMULATION OF THE PROBLEM

We consider a model of a quantum impurity, a small quantum system with a finite number of

bosonic/fermionic degrees of freedom $[d_a, d_b^\dagger]_\pm = \delta_{ab}$ and with Hamiltonian $H_I[d_a, d_a^\dagger]$, coupled to two different quantum baths (see figure 1). We will denote the Hamiltonian of the baths with H_M and $H_{\bar{M}}$, where the subscripts refer to the fact that \bar{M} is a non-Markovian bath and M is a Markovian one. We describe the two environments as a collection of non-interacting bosonic/fermionic modes, (respectively if the impurity is bosonic/fermionic)

$$H_M = \sum_p \omega_p b_p^\dagger b_p \quad H_{\bar{M}} = \sum_k \varepsilon_k c_k^\dagger c_k \quad (1)$$

The total Hamiltonian therefore reads

$$H = H_I + H_M + H_{IM} + H_{\bar{M}} + H_{I\bar{M}}$$

where we have introduced the two coupling terms between the impurity and the M and \bar{M} baths. We will consider the impurity to be *linearly coupled* to the \bar{M} bath, i.e. through a coupling Hamiltonian of the form

$$H_{I\bar{M}} = \sum_{ka} V_{ka} (d_a^\dagger c_{ak} + \text{hc}) \quad (2)$$

while we will not make any assumption at this point on the nature of the coupling between the impurity and the M bath, that could be linear or also include higher powers of the impurity field, i.e.

$$H_{IM} = \sum_{ka} V_{ka}^M (f(d_a, d_a^\dagger) b_{ak} + \text{hc}) \quad (3)$$

with $f(x, y)$ a generic function of the creation/annihilation operator of the impurity.

Defining the time evolution operator of the entire system as $U(t, 0) = e^{-iHt}$ and given an initial condition for the system density matrix $\rho(0)$ we can formally write down the reduced density matrix of the impurity at time t , tracing out the degrees of freedom of the two environments

$$\rho_I(t) = \text{tr}_{M\bar{M}} [U(t, 0)\rho(0)U^\dagger(t, 0)] \quad (4)$$

from which the dynamics of simple impurity observables can be readily obtained as $O_I(t) = \text{tr}[\rho_I(t)O_I]$. With the assumption that the initial density operator of the environment and the impurity factorizes³⁴, we can define the evolution operator of the reduced dynamics

$$\rho_I(t) = \mathcal{V}(t, 0)\rho_I(0) \quad (5)$$

This reduced density operator and its evolution operator are the key quantities over which we will focus our attention throughout the manuscript. Performing the trace over the environment degrees of freedom is a highly non trivial problem. In the following we will obtain two main results. The first one is a formal series from \mathcal{V} to all orders in the coupling with the non-Markovian bath, called hybridization expansion, and the second one is a closed equation for \mathcal{V} , based on a self-consistent resummation of the series.

III. HYBRIDIZATION EXPANSION

In this section we derive a formal hybridization expansion for the reduced density matrix of the impurity. Such an expansion is usually derived in the context of quantum impurity models coupled to a single bath, as a starting point to develop exact Monte-Carlo sampling^{11,35} or approximated resummation techniques^{36,37} to solve the problem. There the formulation is typically done at the level of the partition function, i.e. tracing out also the impurity degrees of freedom, while we are interested in the reduced density matrix and the evolution operator, see Eq. (5) therefore we will not perform such a trace, a fact that will result in some formal difference in the approach. More importantly, here the quantum impurity is also coupled to a second Markovian environment and we will need to trace out this as well in a second stage, under the assumption that the *IM* subsystem obeys a Markovian Lindblad master equation^{34,38}.

A. Tracing Over the Non-Markovian Bath

We begin by performing the trace over the non-Markovian environment which is quadratic in terms of bath operators and linearly coupled to the impurity. Such a trace could be performed exactly within a path integral formulation leading to an effective Keldysh action which is non-local in time. Here we proceed instead at the operator level by noticing that the trace could be taken exactly order by order in an expansion in the coupling between the non-Markovian environment and the impurity.

In order to derive this expansion, we write down the full Hamiltonian of the system as $H = H_0 + H_{\bar{M}} + H_{I\bar{M}}$, describing respectively the impurity embedded in the Markovian bath ($H_0 = H_I + H_M + H_{IM}$), the Non-Markovian environment and its coupling to the impurity. We then move to the interaction picture with respect to the Hamiltonian $H_0 + H_{\bar{M}}$. The density operator becomes

$$\rho(t) = e^{-i(H_0 + H_{\bar{M}})t} T_t e^{-i \int_0^t dt' H_{I\bar{M}}(t')} \rho(0) \times \times \check{T}_t e^{i \int_0^t dt' H_{I\bar{M}}(t')} e^{i(H_0 + H_{\bar{M}})t} \quad (6)$$

We will perform a simultaneous expansion in powers of $H_{I\bar{M}}(t')$ both on the left and on the right of the initial density operator $\rho(0)$. A formal way to manage a single series expansion and to write all the operators on the left side of the density operator, is to use the formalism of the Schwinger/Keldysh double contour $C(t, 0)$ ^{39,40} (fig. 2). Operators on the left (right) side of $\rho(0)$ are assigned a + or - label, so that the couple $(t, \gamma) = t_\gamma$, with $\gamma \in \{+, -\}$, allows to locate one operator on this double time-axis.

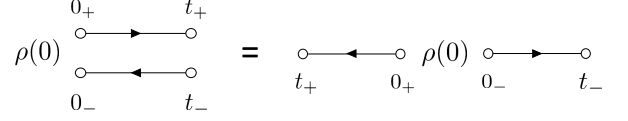


FIG. 2. Two equivalent pictorial representations of the Schwinger/Keldysh contour $C(t, 0)$, describing the non-equilibrium evolution of an initial density operator $\rho(0)$ from time 0 to time t . The two branches of the contour are usually called + and - and they correspond to the two time evolution operators applied to the left and to the right of the initial density operator, as in eq. (6).

We introduce the standard Keldysh time-ordering on the contour as follows:

$$t_\gamma > t'_{\gamma'} \quad \text{if} \quad \begin{cases} t > t' & \gamma = \gamma' = + \\ t < t' & \gamma = \gamma' = - \\ \gamma = - & \gamma' = + \end{cases} \quad (7)$$

This ordering allows to define a time-ordering operator T_C , such that two operators, X_1 and X_2 , being X a creation or annihilation fermionic (bosonic) operator, anticommute (commute) under time-ordering: $T_C X_1(t_\gamma) X_2(t_{\gamma'}) = \xi T_C X_2(t_{\gamma'}) X_1(t_\gamma)$, with

$$\begin{aligned} \xi &= 1 & \text{for bosons} \\ \xi &= -1 & \text{for fermions} \end{aligned}$$

The time ordering operator is defined as follows

$$T_C X_1(t_\gamma) X_2(t_{\gamma'}) = \begin{cases} X_1(t_\gamma) X_2(t_{\gamma'}) & \text{for } t_\gamma > t'_{\gamma'} \\ \xi X_2(t_{\gamma'}) X_1(t_\gamma) & \text{for } t_\gamma < t'_{\gamma'} \end{cases} \quad (8)$$

which naturally extends to the case of n operators. Once time ordered, the operators belonging to the - branch of the contour have to be brought on the right side of the density matrix, as if there we were exploiting the cyclic property of a trace.

By defining contour integrals as $\int_{C(0,t)} dt \equiv \int_0^{t_+} dt_+ - \int_0^{t_-} dt_-$, one can show that the density operator evolution (6) can be written in the compact form

$$\rho(t) = T_C e^{-i(H_0 + H_{\bar{M}})(t_+ - t_-)} e^{-i \int_{C(0,t)} dt' H_{I\bar{M}}(t')} \rho(0) \quad (5)$$

and, accordingly, the evolution operator defined in (5) can be written as

$$\mathcal{V}(t, 0) \rho_I(0) = \text{tr}_{M\bar{M}} \left[T_C e^{-iH_0(t_+ - t_-)} e^{-i \int_{C(0,t)} dt' H_{I\bar{M}}(t')} \rho(0) \right] \quad (9)$$

In order to perform the partial trace on the non-Markovian environment, we assume that at time $t = 0$ there's no entanglement between the non-Markovian bath and the rest of the system, such that the density operator factorizes $\rho(0) = \rho_{IM}(0) \otimes \rho_{\bar{M}}(0)$, with $\rho_{\bar{M}}(0)$ quadratic in bosonic/fermionic operators. Initial entangled states could be taken into account considering

a third, imaginary time branch of the non-equilibrium contour^{41–43}, but this is beyond the interest of this work.

We then Taylor-expand the time-ordered exponential in power of the impurity-bath hybridization $H_{I\bar{M}}$ and perform the trace over the bath degrees of freedom, which immediately reduces the expansion to only even order terms. Then using Wick's theorem and performing the sums over $\{b_i, b'_i\}$, we can write the final result in terms

of the bath hybridization function

$$\Delta_{a'a}(t', t) \equiv \sum_{b'} V_{a'b'} V_{ab'}^* G_{b'}(t', t) \quad (10)$$

where $G_{b'}(t', t) = -i\langle T_C c_{b'}(t') c_{b'}^\dagger(t) \rangle$ is the contour ordered bath Green's function. Finally, we obtain the hybridization expansion^{35,36,44}:

$$\begin{aligned} \mathcal{V}(t, 0) [\rho_I(0)] &= \sum_{k=0} \frac{(-i)^k}{k!^2} \sum_{\gamma_1 \dots \gamma'_k} \prod_i \gamma_i \gamma'_i \sum_{a_1 \dots a'_k} \int_0^t dt_1 \dots \int_0^t dt'_k \text{tr}_M \left[T_C e^{-iH_0(t_+ - t_-)} d_{a'_k}^\dagger(t'_k, \gamma'_k) d_{a_k}(t_k, \gamma_k) \dots d_{a_1}(t_1, \gamma_1) \rho_{IM}(0) \right] \times \\ &\times \sum_{\sigma \in P} \xi^{\text{sign}(\sigma)} \Delta_{a'_1 a_{\sigma(1)}}^{\gamma'_1 \gamma_{\sigma(1)}}(t'_1, t_{\sigma(1)}) \dots \Delta_{a'_k a_{\sigma(k)}}^{\gamma'_k \gamma_{\sigma(k)}}(t'_k, t_{\sigma(k)}) \end{aligned} \quad (11)$$

γ_i, γ'_i are contour indices $\gamma \in \{+, -\}$. We notice that the hybridization function $\Delta_{a'_i a_{\sigma(i)}}^{\gamma'_i \gamma_{\sigma(i)}}(t'_i, t_{\sigma(i)})$ connects the $d_{a_{\sigma(i)}}(t_{\sigma(i)})$ operator with the $d_{a'_i}^\dagger(t'_i)$ one. We can interpret this construction as follows. The d operator creates a "hole" in the impurity, which is propagated through the system and then annihilated by a d operator. To this hole it corresponds (from the definition of Δ) a particle of the environment which is created, propagated and annihilated. Thus, the series eventually describes processes in which particles hop from the impurity to the environment and back to the impurity.

B. Tracing over the Markovian bath

1. Super-operators formalism

It is useful to describe time-evolution using super-operators, as these are natural objects to describe the dynamics of open systems and since they provide a useful framework to work out the trace on the Markovian environment in eq. (11). We call super-operator an operator that acts on an operator, rather than on quantum state. We denote super-operators with calligraphic letters. The focus is shifted from the standard evolution operator $U(t, 0) = e^{-iHt}$, which evolves a pure state (a ket) in time, to the super-operator $\mathcal{U}(t, 0)$ which time-evolves a density operator and is defined by

$$\rho(t) = U(t, 0) \rho(0) U(0, t) \equiv \mathcal{U}(t, 0) \rho(0) \quad (12)$$

We can write a generic time-ordered string of operators, like it appears in eq. (11), in the Schrödinger's picture and in a compact form, using the super-operators notation. This comes at the price of introducing some notation.

We promote d, d^\dagger operators in the Schrödinger's picture to super-operators $\mathcal{D}_\gamma, \mathcal{D}_\gamma^\dagger$, with an contour index γ

reminiscent of the branch the original operators belonged to:

$$\mathcal{D}_\gamma^{(\dagger)}[\bullet] = \begin{cases} d^{(\dagger)} \bullet & \text{if } \gamma = + \\ \bullet d^{(\dagger)} & \text{if } \gamma = - \end{cases} \quad (13)$$

We trivially generalize the contour time-ordering operator T_C to the super-operators notation

$$\begin{aligned} T_C X_{1(t, \gamma)} \mathcal{U}_0(t, t') X_{2(t', \gamma')} &= \\ &= \begin{cases} X_{1(t, \gamma)} \mathcal{U}_0(t, t') X_{2(t', \gamma')} & \text{for } (t, \gamma) > (t', \gamma') \\ \xi X_{2(t', \gamma')} \mathcal{U}_0(t', t) X_{1(t, \gamma)} & \text{for } (t, \gamma) < (t', \gamma') \end{cases} \end{aligned} \quad (14)$$

The $X_{t, \gamma}$ super-operators are objects in Schrödinger's picture and their time label t is just meant to know how to order them.

We also need to introduce a further "forward" time-ordering operator T_F , that orders two super-operators according to their time labels t, t' , regardless of their contour index:

$$\begin{aligned} T_F X_{1(t, \gamma)} \mathcal{U}_0(t, t') X_{2(t', \gamma')} &= \\ &= \begin{cases} X_{1(t, \gamma)} \mathcal{U}_0(t, t') X_{2(t', \gamma')} & \text{for } t > t' \\ X_{2(t', \gamma')} \mathcal{U}_0(t', t) X_{1(t, \gamma)} & \text{for } t < t' \end{cases} \end{aligned} \quad (15)$$

This definition is the same for both fermions and bosons, with no extra minus signs for fermions.

Using these definitions, we can write the following identity

$$\begin{aligned} T_C e^{-iH_0(t_+ - t_-)} d^\dagger(t'_k) \dots d(t_1) \rho_{IM}(0) &= \\ = T_F T_C \mathcal{U}_0(t, t'_k) \mathcal{D}_{t'_k \gamma'_k}^\dagger \mathcal{U}_0(t'_k, t_{k-1}) \dots \mathcal{D}_{t_1 \gamma_1} \mathcal{U}_0(t_1, 0) \rho_{IM}(0) \end{aligned} \quad (16)$$

The second line is a chain of subsequent time-evolutions operated by \mathcal{U}_0 , going overall from time 0 to

time t , alternated with the application of $\mathcal{D}, \mathcal{D}^\dagger$ super-operators. We remark that the two time-order operators T_C and T_F do not commute. In order to evaluate the second line of eq. (16), one has first to order the super-operators according to T_C ; this first ordering is necessary in order to compute the non-trivial sign factor obtained by swapping fermionic operators. Then the super-operators must be re-ordered according to the "forward" time-ordering operator T_F . This insures that, in order to evaluate eq. (16), one has to apply only forward in time evolution super-operators.

2. Performing the partial trace

We now aim at performing the partial trace on the Markovian environment which is left in eq. (11). This trace is taken on a contour time-ordered string of impurity operators. The latter are nevertheless evolved by the joint dynamics of the impurity plus the remaining bath, making the partial trace non trivial to evaluate. In⁴⁵ the authors showed that, assuming that the impurity-bath dynamics is governed by a Lindblad master equation, then the partial trace becomes trivial. We report a proof here as this is a crucial step to obtain the hybridization expansion (21). We recall the Lindblad master equation^{34,38}:

$$\partial_t \rho_I^0 = -i [H_I, \rho_I^0] + \sum_{\alpha} \gamma_{\alpha} \left(L_{\alpha} \rho_I^0 L_{\alpha}^{\dagger} - \frac{1}{2} \{ L_{\alpha}^{\dagger} L_{\alpha}, \rho_I^0 \} \right) \quad (17)$$

where L_{α} are the jump operators, microscopically determined by the environment-impurity coupling (3). $\rho_I^0(t)$ must not be confused with $\rho_I(t) = \text{tr}_M \rho_{IM}(t)$, as the former is the density operator obtained by evolving $\rho(0)$ in presence of the Markovian environment alone. $\rho_I(t)$ instead is obtained by evolving $\rho(0)$ with a dynamics

that includes both the Markovian and non-Markovian environments. Defining the Markovian evolution super-operator, $\mathcal{V}_0(t - t') = e^{\mathcal{L}(t-t')}$, with $t > t'$, then

$$\rho_I^0(t) = \mathcal{V}_0(t - t') \rho_I(0) \quad (18)$$

We remark that \mathcal{V}_0 depends only on time differences as it satisfies (17). This is equivalent to

$$\text{tr}_M \rho_{IM}^0(t) = \text{tr}_M [\mathcal{U}_0(t, t') \rho_{IM}^0(t')] = \mathcal{V}_0(t - t') \text{tr}_M \rho_{IM}^0(t') \quad (19)$$

In order to show how to perform the trace of the string of super-operators in (16), let's assume time ordering is already enforced so that we don't have to care about it. Defining $r_1(t) = \mathcal{U}_0(t, t'_k) r_1(t'_k)$ and $r_1(t'_k) = d_{t'_k \gamma'_k}^{\dagger} \mathcal{U}_0(t'_k, t_{k-1}) \dots d_{t_1 \gamma_1} \mathcal{U}_0(t_1, 0) \rho_{IM}(0)$, we can break down the tracing operation as follows:

$$\begin{aligned} \text{tr}_M [\mathcal{U}_0(t, t'_k) \mathcal{D}_{t'_k \gamma'_k}^{\dagger} \dots \mathcal{D}_{t_1 \gamma_1} \mathcal{U}_0(t_1, 0) \rho_{IM}(0)] &= \\ \text{tr}_M r_1(t) &= \text{tr}_M [\mathcal{U}_0(t, t'_k) r_1(t'_k)] = \mathcal{V}_0(t - t') \text{tr}_M r_1(t'_k) \end{aligned} \quad (20)$$

The last equality is analogous to eq. (19) and holds under the same assumptions leading to Lindblad master equation. One can iterate this procedure, as now $\text{tr}_M r_1(t'_k) = \mathcal{D}_{t'_k \gamma'_k}^{\dagger} \text{tr}_M [\mathcal{U}_0(t'_k, t_{k-1}) r_2(t_{k-1})]$, to turn all the \mathcal{U}_0 super-operators in eq. (11) in \mathcal{V}_0 ones.

3. Generalized hybridization expansion

We then get to the final form of the hybridization expansion in presence of both a non-Markovian and Markovian environment, that is one of the main results of this work:

$$\begin{aligned} \mathcal{V}(t, 0) &= \sum_{k=0} \frac{(-i)^k}{k!^2} \sum_{\gamma_1 \dots \gamma'_k} \prod_i \gamma_i \gamma'_i \sum_{a_1 \dots a'_k} \int_0^t dt_1 \dots \int_0^t dt'_k T_F T_C \mathcal{V}_0(t, t'_k) \mathcal{D}_{a'_k (t'_k \gamma'_k)}^{\dagger} \mathcal{V}_0(t'_k, t_{k-1}) \dots \mathcal{D}_{a_1 (t_1 \gamma_1)} \mathcal{V}_0(t_1, 0) \times \\ &\times \sum_{\sigma \in P} \xi^{\text{sign}(\sigma)} \Delta_{a'_1 a_{\sigma(1)}}^{\gamma'_1 \gamma_{\sigma(1)}}(t'_1, t_{\sigma(1)}) \dots \Delta_{a'_k a_{\sigma(k)}}^{\gamma'_k \gamma_{\sigma(k)}}(t'_k, t_{\sigma(k)}) \end{aligned} \quad (21)$$

This series can be sampled using stochastic sampling techniques^{11,35,46} or approximately resummed^{36,37}. For both purposes, it is useful to define the Feynman rules for the series (21).

4. Matrix representation

Each term of the hybridization expansion (21) must be understood as a composition of applications of super-operators, from the right-most to the left-most one, on the initial density operator. We remark that in the usual representation in which states of the Hilbert space are vectors and operators are matrices, super-operators are rank-4 tensors. Instead, if we write operators as vectors,

then super-operators become matrices. This is convenient to evaluate terms of the hybridization expansion (21) as matrix products. Namely

$$\begin{aligned} & \mathcal{V}_0(t, t'_k) \mathcal{D}_{a'_k(t'_k \gamma'_k)}^\dagger \cdots \mathcal{D}_{a_1(t_1 \gamma_1)} \mathcal{V}_0(t_1, 0) \rho_I(0) \\ & \rightarrow \bar{\bar{\mathcal{V}}}_0(t, t'_k) \bar{\bar{\mathcal{D}}}_{a'_k(t'_k \gamma'_k)}^\dagger \cdots \bar{\bar{\mathcal{D}}}_{a_1(t_1 \gamma_1)} \bar{\bar{\mathcal{V}}}_0(t_1, 0) |\rho_I(0)\rangle \end{aligned} \quad (22)$$

using double bars to indicate matrices. Operators are represented as vectors in a space which is the tensor product (indicated with \otimes) of two copies of the original Hilbert space. The vectorization procedure, taking the example of the density operator, reads:

$$\rho = \sum_{n,m} \rho_{nm} |n\rangle \langle m| \rightarrow \sum_{n,m} \rho_{nm} |n\rangle \otimes |m\rangle \equiv |\rho\rangle \quad (23)$$

The matrices $\bar{\bar{\mathcal{V}}}, \bar{\bar{d}}, \bar{\bar{d}}^\dagger$ corresponding to the super-operators $\mathcal{V}, d, d^\dagger$ are defined by the following simple procedure. Let's consider the super-operator $\mathcal{S} \bullet = A \bullet B$. Representing ρ as a vector $|\rho\rangle$, then also $\mathcal{S}\rho$ will be a represented as a vector according to eq. (23). It's simple to show that $|\mathcal{S}\rho\rangle = \bar{\bar{\mathcal{S}}}|\rho\rangle$ defining $\bar{\bar{\mathcal{S}}} = \bar{\bar{A}} \otimes \bar{\bar{B}}^T$. The matrix form of $\mathcal{D}_\pm, \mathcal{D}_\pm^\dagger$ in the doubled Hilbert space is

$$\begin{aligned} \bar{\bar{\mathcal{D}}}_+ &= \bar{\bar{d}} \otimes \bar{\mathbb{1}} & \bar{\bar{\mathcal{D}}}_+^\dagger &= \bar{\bar{d}}^\dagger \otimes \bar{\mathbb{1}} \\ \bar{\bar{\mathcal{D}}}_- &= \bar{\mathbb{1}} \otimes \bar{\bar{d}}^T & \bar{\bar{\mathcal{D}}}_-^\dagger &= \bar{\mathbb{1}} \otimes \bar{\bar{d}}^* \end{aligned}$$

with $\bar{\bar{\mathcal{D}}}_\pm^\dagger$ the hermitian conjugate of $\bar{\bar{\mathcal{D}}}_\pm$. These rules allow to obtain the matrix representation of the Liouvillian and then of \mathcal{V}_0 .

C. Feynman Rules

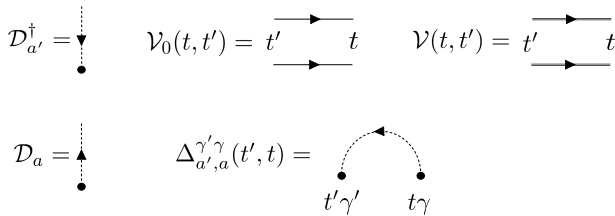


FIG. 3. The Feynman rules to represent the hybridization expansion (21). The arrow of the hybridization line Δ goes from a \mathcal{D} super-operator to the first a \mathcal{D}^\dagger one.

the Feynman rules to draw the hybridization expansion (21) are represented in figure 3. We will use these rules to draw a term with $2k$ annihilation and creation super-operators, with a particular ordering for the times $\{t_i, t'_i \dots t_1, t'_1\}$ and a choice of a permutation $\{\sigma(1), \sigma(2) \dots \sigma(k)\}$. To do that, we draw a couple of

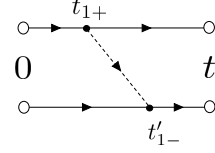


FIG. 4. The Feynman diagram representing eq. (24)

parallel axes representing the double contour from time $t = 0$ to time t . \mathcal{D}_γ ($\mathcal{D}_\gamma^\dagger$) super-operators are represented as a dashed half-line with outwards (inwards) arrows, stemming from the contour branch γ . The dashed half-lines corresponding to the super-operators $\mathcal{D}_{a'_i(t'_i \gamma'_i)}^\dagger$ and $\mathcal{D}_{a_{\sigma(i)}(t_{\sigma(i)} \gamma_{\sigma(i)})}$ are joined together to form a hybridization line, representing the hybridization function $\Delta_{a'_i a_{\sigma(i)}}^{\gamma'_i \gamma_{\sigma(i)}}(t'_i, t_{\sigma(i)})$, which has an arrow going from \mathcal{D} to \mathcal{D}^\dagger . Then, each part of the double contour between two integration times, drawn as two parallel solid segments, represents a time-propagation super-operator \mathcal{V}_0 . The dressed evolution operator \mathcal{V} is drawn by replacing the contour solid lines by double lines. As an example, the diagram corresponding to

$$i \int_0^t dt_1 \int_0^{t_1} dt'_1 \mathcal{V}_0(t, t'_1) \mathcal{D}_{a'_1}^\dagger \mathcal{V}_0(t'_1, t_1) \mathcal{D}_{a_1} \mathcal{V}_0(t_1, 0) \Delta_{a'_1, a_1}^{+, -}(t'_1, t_1) \quad (24)$$

is shown in figure 4. All the diagrams with $2k$ annihilation and creation super-operators are generated by connecting \mathcal{D}^\dagger super-operators to \mathcal{D} ones in all possible choices of permutations σ and considering all possible time orderings of integration times.

IV. SELF-CONSISTENT DIAGRAMMATIC RESUMMATIONS TECHNIQUES

In this section we start from the hybridization expansion derived in section III, which involves bare diagrams to all orders, and use the Feynman rules to introduce diagrammatic resummation techniques.

To proceed further it is useful to draw more compact diagrams where the double contour is collapsed on a single time-axis and thus a time propagation \mathcal{V}_0 is represented by a single line, as we show in figure 5. These compact diagrams represent an ensemble of diagrams drawn with the rules we introduced in 3.

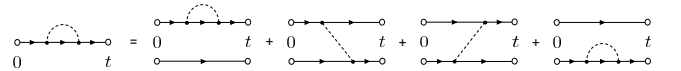


FIG. 5. Compact diagrams represent an ensemble of diagrams hiding the double contour structure. By omitting the arrows on hybridization lines, we mean that all the possible choices must be considered.

The advantage of this notation is that all the diagrams represented by a single compact diagram have the same

topology in terms of being 1-particle irreducible or non-crossing. Figure 6 shows the hybridization expansion drawn using these compact diagrams.

A. Dyson Equation

As a first step it is useful to distinguish diagrams which are one-particle irreducibles, i.e. compact diagrams which cannot be separated, by cutting a solid line, in two parts that are not connected by any hybridization line, as indicated in figure 6. Then, we introduce the self-energy Σ as the sum of one particle irreducible (1PI) diagrams. All the non-1PI diagrams can be obtained by joining some 1PI diagrams with solid lines, thus the whole series can be written as

$$\mathcal{V} = \mathcal{V}_0 + \mathcal{V}_0 \circ \Sigma \circ \mathcal{V}_0 + \mathcal{V}_0 \circ \Sigma \circ \mathcal{V}_0 \circ \Sigma \circ \mathcal{V}_0 + \dots$$

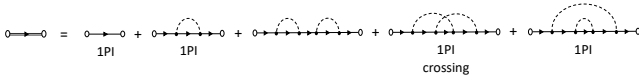


FIG. 6. 1PI diagrams of the hybridization expansion in eq. (21)

We remark that the objects composing this series, \mathcal{V}_0 and Σ , are super-operators and the series must be understood as a composition of applications of super-operators, from the right-most to the left-most one, on a target operator. Self-energies and propagators are joined by the circle operation, standing for a super-operator application and a partial time convolution. Using brackets to stress that we refer to a super-operator application and the symbol \bullet to indicate a target operator, we have

$$\Sigma(t, t_1) \circ \mathcal{V}_0(t_1, t') \equiv \int_{t'}^t dt_1 \Sigma(t, t_1) [\mathcal{V}_0(t_1, t') \bullet]$$

The series above sums up to the Dyson equation

$$\begin{aligned} \mathcal{V}(t, t') &= \mathcal{V}_0(t, t') + \int_{t'}^t dt_1 \int_{t'}^{t_1} dt_2 \mathcal{V}_0(t, t_1) \Sigma(t_1, t_2) \mathcal{V}(t_2, t') \\ &= \mathcal{V}_0(t, t') + \int_{t'}^t dt_1 \int_{t'}^{t_1} dt_2 \mathcal{V}(t, t_1) \Sigma(t_1, t_2) \mathcal{V}_0(t_2, t') \end{aligned} \quad (25)$$

$$\Sigma(t_1, t_2) = \sum_{a,b} \sum_{\alpha\beta \in \{+,-\}} -\alpha^{(1+\xi)/2} \beta i \left[\Delta_{ba}^{\beta\alpha}(t_1, t_2) \mathcal{D}_{\beta b}^\dagger \mathcal{V}(t_1, t_2) \mathcal{D}_{\alpha a} + \xi \Delta_{ab}^{\alpha\beta}(t_2, t_1) \mathcal{D}_{\beta b} \mathcal{V}(t_1, t_2) \mathcal{D}_{\alpha a}^\dagger \right] \quad (26)$$

where $\alpha, \beta \in \{+, -\}$ are contour indices, a, b are the fermionic generic indices.

We can interpret the two terms in eq. (26) as follows. The first term propagates a hole in the impurity (applies

B. The Non-Crossing Approximation

The non-crossing approximation (NCA) corresponds to approximating the series for \mathcal{V} , and thus also for Σ , by considering only the compact diagrams in which the hybridization lines do not cross³⁷. The NCA diagrams composing the self-energy are shown in figure 7.

$$\Sigma = \text{diagram 1} + \text{diagram 2} + \text{diagram 3} + \text{diagram 4} = \text{diagram 5}$$

FIG. 7. The NCA series of the self-energy Σ . The resummed series for Σ corresponds to its $k = 1$ diagrams, where the bare propagator \mathcal{V}_0 is replaced with the dressed one \mathcal{V} .

In order to prove the second equality in figure 7, we remark that the first and last times of a self-energy diagram must be connected together by an hybridization line. If it's not the case, in fact, the resulting diagram is either non-1PI or it's crossed. Then all the diagrams of Σ (in NCA) are obtained connecting the intermediate times to form all the possible non-crossing diagrams, (not only the 1PI ones this time). But the latter diagrams in turn define the NCA series for \mathcal{V} . This proves the second equality in figure 7. We remark that then, the NCA self-energy coincides with its contributions (with $k = 1$), where the bare propagator \mathcal{V}_0 is replaced with the dressed one \mathcal{V} .

To obtain an analytic expression of the self-energy, we have to cast the $k = 1$ term of the hybridization expansion (21) in a form in which the innermost integration time is lower than the outermost, that is with integrals of the form $\int_{t'}^t dt_1 \int_{t'}^{t_1} dt_2$. In doing so, one must deal with the signs coming out of the time ordering. We report the calculation in the supplementary material.

The expression for the self-energy eventually reads

\mathcal{D}^\dagger first and then \mathcal{D}) and a particle in the bath, the latter being described by a hybridization function with the same time arguments of \mathcal{V} ; The second term propagates a particle in the impurity and a hole in the bath with

a hybridization function with opposite time arguments than \mathcal{V} .

We remark that the self-energy (26) we obtained here is formally similar to what one obtains in imaginary time for equilibrium applications (eq. (12) of³⁷), with the difference that we have super-operators and a Keldysh contour structure. In contrast with other non-equilibrium NCA works^{47,48}, we worked on a two-branches, instead of three-branches, non-equilibrium contour and, as a consequence we obtained a single Dyson equation for the super-operator $\mathcal{V}(t, t')$, instead of 3 coupled Dyson equations plus 1 uncoupled one. On the other hand, $\bar{\mathcal{V}}(t, t')$ is an $N^2 \times N^2$ matrix, while the Dyson equations in^{47,48} involve $N \times N$ matrices. We remark that our super-operators approach to the hybridization expansion, that was necessary to deal with the additional Markovian environment, could be used as well in its absence. The expressions for the hybridization expansion (21) and the NCA equations (25),(26), would be unchanged, apart from replacing $\mathcal{V}(t, t')$ and $\mathcal{V}_0(t, t')$ with $\mathcal{U}(t, t')$ and $\mathcal{U}_0(t, t')$.

C. Properties of the NCA propagator

The propagator $\mathcal{V}(t, t')$ obtained in NCA is the time-evolution super-operator of the reduced density operator of the impurity. Assuming to switch on the interaction with the non-Markovian bath at time $t = 0$, then the density operator of the impurity at time t is given by $\rho_I(t) = \mathcal{V}(t, 0)\rho_I(0)$. A time evolution super-operator, must be a convex-linear, completely positive and trace-preserving map. We refer to³⁴ for a precise definition of these properties. It is natural to ask which of these properties are preserved by the NCA approximation. It's trivial to show that \mathcal{V} is a linear map, implying it is also convex linear. We can also prove that it is trace-preserving. We stress that $\mathcal{V}(t, t')$ describes a non-Markovian evolution, so it does not form a semi-group, that is $\mathcal{V}(t, t') \neq \mathcal{V}(t, t_1)\mathcal{V}(t_1, t')$ with $t' < t_1 < t$. Time-evolution super-operators have also interesting spectral properties following from trace preservation. We call $\lambda_i(t, t')$, $v_i^R(t, t')$, $v_i^L(t, t')$ the eigenvalues and right and left eigenvectors of $\mathcal{V}(t, t')$, which depend on time. As it preserves the trace, $\mathcal{V}(t, t')$ must have at least one eigenvalue equal to one, say $\lambda_0 \equiv 1$. In fact $\text{tr}[\mathcal{V}(t, t')\rho] = \text{tr}[\rho]$ in the matrix notation reads $\langle \mathbb{1} | \bar{\mathcal{V}}(t, t') | \rho \rangle = \langle \mathbb{1} | \rho \rangle$ which holds for every $|\rho\rangle$; then $\langle \mathbb{1} |$ must be a left eigenvector of $\mathcal{V}(t, t')$, $\langle v_0^L | \equiv \langle \mathbb{1} |$, with eigenvalue $\lambda_0 \equiv 1$. If we assume that there is only one eigenvector with eigenvalue 1, corresponding to a right-eigenvector with non-zero trace: $\langle \mathbb{1} | v_i^R(t, t') \rangle = \text{tr}[v_i^R(t, t')] = 0$, for $i \neq 0$. We will explicitly check these properties in the next section, when we will apply our NCA algorithm to a specific example.

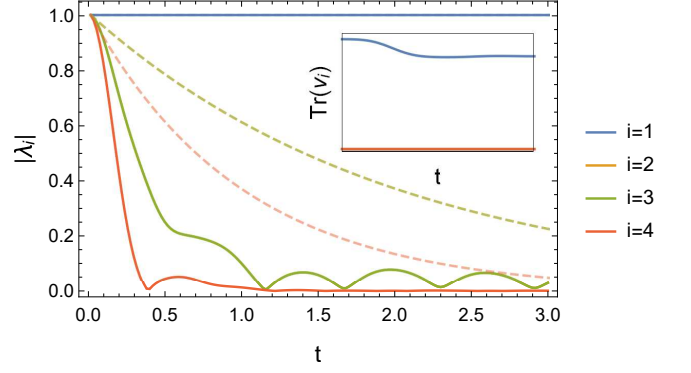


FIG. 8. Real-time evolution of the absolute value of the eigenvalues of the impurity propagator. While an eigenvector with eigenvalue one is present at all times, all the other eigenvalues decay to zero at long times. The $i = 2$ and $i = 3$ curves coincide because the corresponding eigenvalues are complex conjugates. The decay is purely exponential for a Markovian system while strong deviations appear in the non-Markovian case. Parameters: $\epsilon_0 = 5$, $\gamma = \gamma_l = \gamma_p = \gamma_d = 0.5$, $w = 10$, $\eta = 1$, $\Delta t = 0.02$, $\rho_0 = |0\rangle\langle 0|$.

V. CASE STUDY: SPIN-LESS FERMIONIC IMPURITY

As a non trivial application of the NCA approach for open system described so far, we consider here a model of a single-mode, spin-less fermionic impurity with Markovian losses, pump and dephasing and further coupled to a non-Markovian fermionic environment, as described in equation (1). The Markovian dynamics is described by a Lindblad master equation

$$\begin{aligned} \partial_t \rho_I^0 &= \mathcal{L} \rho_I^0 \\ \mathcal{L} \rho_I^0 &= -i [H_I, \rho_I^0] + (\gamma_l \mathcal{D}_l + \gamma_p \mathcal{D}_p + \gamma_d \mathcal{D}_d) \rho_I^0 \\ H_I &= \epsilon_0 d^\dagger d \\ \mathcal{D}_l \rho_I^0 &= d \rho_I^0 d^\dagger - \frac{1}{2} \{d^\dagger d, \rho_I^0\} \\ \mathcal{D}_p \rho_I^0 &= d^\dagger \rho_I^0 d - \frac{1}{2} \{d d^\dagger, \rho_I^0\} \\ \mathcal{D}_d \rho_I^0 &= d^\dagger d \rho_I^0 d^\dagger d - \frac{1}{2} \{d^\dagger d, \rho_I^0\} \end{aligned}$$

where ϵ_0 is the energy of the fermionic level.

The effect of the non-Markovian environment on the impurity is completely determined by its hybridization function (10). Here we choose a zero temperature, particle hole symmetric, fermionic bath with constant density of states of bandwidth $2W$ and with coupling strength to the impurity η . As a result the hybridization function depends only on time-differences. As a consequence, also \mathcal{V} depends only on time differences and we will set $t' = 0$ for convenience in the following. With these definitions

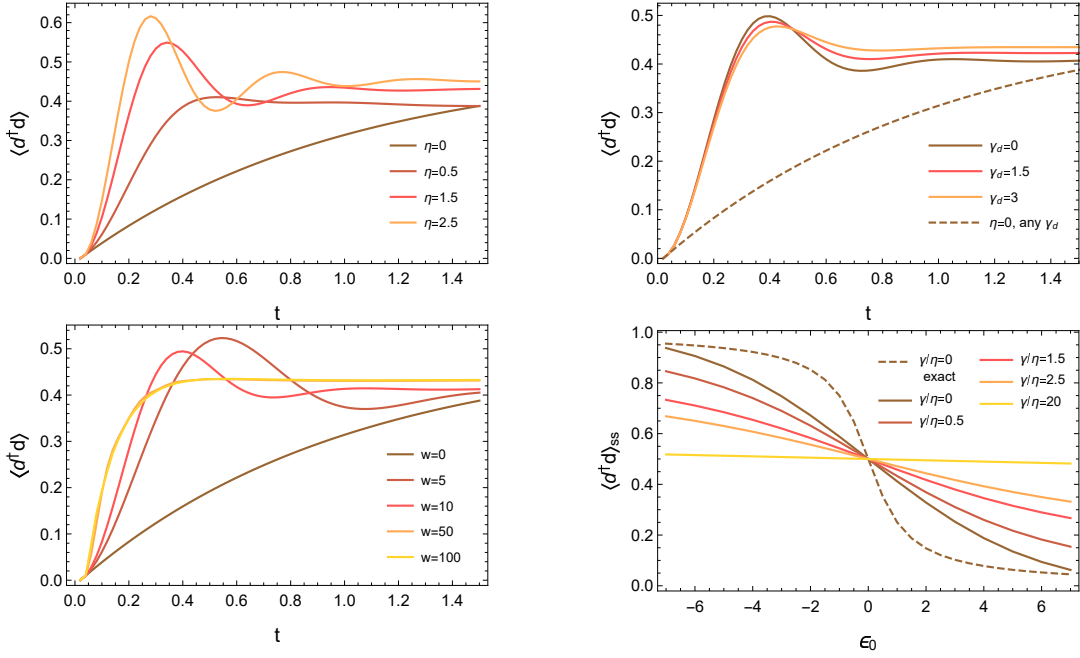


FIG. 9. Dynamics of the number of fermions for different sets of parameters, namely changing the hybridization strength (Top left) the bandwidth (bottom left) and the dephasing rate (top right). Average population of the stationary state as a function of the energy level (bottom right). Parameters: $\epsilon_0 = 1$, $\gamma = \gamma_l = \gamma_p = \gamma_d = 0.5$, $w = 10$, $\eta = 1$, $\Delta t = 0.02$, $\rho_0 = |0\rangle\langle 0|$.

we get for the hybridization functions

$$\begin{aligned}\Delta^{+-}(t) &= 2i\eta e^{iwt/2} \sin(wt/2)/t \\ \Delta^{-+}(t) &= -2i\eta e^{-iwt/2} \sin(wt/2)/t\end{aligned}$$

To solve the Dyson equation (25) numerically, we write it in the integro-differential form

$$\partial_t \mathcal{V}(t) = \mathcal{L}\mathcal{V}(t) + \int_0^t dt_1 \Sigma(t-t_1) \mathcal{V}(t_1) \quad (27)$$

that is equivalent to eq. (25), which we solve using the simple discretization scheme $\partial f(t) = [f(t+\Delta t) - f(t)]/\Delta t$, $\int_0^t dt_1 f(t_1) = \Delta t/2 \sum_{l=0}^{t/\Delta t-1} [f((l+1)\Delta t) + f(l\Delta t)]$, with time-step Δt . More refined integration methods are explained in detail in³⁶. The Hilbert space of the impurity has size $N = 2$, so that the super-operator \mathcal{V} has size $N^2 \times N^2 = 4 \times 4$.

A. Results

We start analyzing the spectral properties of the propagator $\mathcal{V}(t)$, which have been discussed generically in the previous section, and are reported in figure 8. In particular we plot the time dependence of the eigenvalues, both in the purely Markovian case (dashed lines) as well in presence of both kind of dissipations. We notice that in both cases there is an eigenvalue which remains equal to

one, while the others decay to zero at long times. However the nature of this decay is rather different in the two cases, showing a much faster dynamics and long time oscillations in the non-Markovian case as opposed to a pure exponential decay in the Markovian one.

We then consider the dynamics of a simple observable, such as the density of fermions in the impurity level, as a function of time and for different parameters (see panel figure 9). In the left figures we plot the dynamics for different values of the coupling η (top) and bandwidth w (bottom) of the non-Markovian environment, in presence of fixed Markovian losses, pump and dephasing. We see that with respect to the purely Markovian dynamics, characterized by a simple exponential relaxation, the NCA approach captures important aspects related to the non-Markovian nature of the environment. In particular the dynamics becomes characterized by oscillations whose amplitude and frequency increase with the coupling η . Similarly, changing the bandwidth of the non-Markovian bath also induces damped oscillations in the evolution, which however disappear in the large bandwidth limit when an exponential relaxation is recovered. Overall we can notice that the Non-Markovian environment makes the dynamics substantially faster. For what concerns the stationary state, we notice from the bottom right plot that the average density would be independent on the energy position in the purely Markovian case, which mimics an infinite temperature fully mixed stationary state. As opposite the coupling to the non-Markovian bath makes the population depend strongly on the position of the energy level and gives a result

which is in good agreement with the theoretical expectation, although we stress that for the non-interacting model we consider here the NCA approximation, which is based on a strong coupling expansion, is not expected to be exact. Finally we also study the role of dephasing: in the purely Markovian model this would not affect the average density of the impurity while the coupling to the non-Markovian bath makes a small dependence visible.

VI. CONCLUSIONS

In this work we have focused on a model for a quantum impurity coupled simultaneously to a Markovian and a non-Markovian environment. We derived a formal hybridization expansion for the evolution super-operator of the impurity, obtained after tracing out all the bath degrees of freedom. This result generalizes to the non-unitary case the hybridization expansion obtained for quantum impurity models. As such it provides the natural starting point for the development of stochastic sampling techniques of the dissipative real-time dynamics of the impurity based on Diagrammatic Monte Carlo, that we leave for future studies. Starting from this expansion we define real-time diagrammatic rules and write down a Dyson Equation for the impurity propagator that we evaluate retaining only non-crossing diagrams, an approximation which is known to capture some aspects of the impurity physics at strong coupling. The resulting approach leads to a trace and hermiticity preserving Non-Markovian dynamical map, with consequences on the spectral properties of the evolution super-operator, while proving its positivity in full generality remains an open question.

As an application, we solved numerically the Dyson equation for the simple model of a fermionic, single-mode impurity, with Markovian losses, pump and dephasing and a non-Markovian, zero temperature environment. This model is non-trivial for the presence of dephasing, which is a quartic term in fermionic operators. This simple implementation allowed to check the spectral properties of the evolution super-operator and to study how Markovian dynamics gets modified by coupling to a non-Markovian environment. Future directions include the exploration of more complex impurity models involving internal degrees of freedom such as the Anderson Impurity model, as well as bosonic extensions and to use of this method as an impurity solver within a dynamical mean field theory approach to driven-dissipative systems.

¹A. O. Caldeira and A. J. Leggett, “Influence of dissipation on quantum tunneling in macroscopic systems,” *Phys. Rev. Lett.* **46**, 211 (1981).

²A. J. Leggett, S. Chakravarty, A. T. Dorsey, M. P. A. Fisher, A. Garg, and W. Zwerger, “Dynamics of the dissipative two-state system,” *Rev. Mod. Phys.* **59**, 1 (1987).

³K. L. Hur, L. Henriët, L. Herviou, K. Plekhanov, A. Petrescu, T. Goren, M. Schiró, C. Mora, and P. P. Orth, “Driven dissipative dynamics and topology of quantum impurity systems,”

Comptes Rendus Physique **19**, 451 – 483 (2018), quantum simulation / Simulation quantique.

⁴A. C. Hewson, *The Kondo Problem to Heavy Fermions* (Cambridge University Press, 1993).

⁵D. Goldhaber-Gordon *et al.*, “Kondo effect in a single-electron transistor,” *Nature* **391**, 156 (1998).

⁶M. Grobis, I. G. Rau, R. M. Potok, H. Shtrikman, and D. Goldhaber-Gordon, “Universal Scaling in Nonequilibrium Transport through a Single Channel Kondo Dot,” *Phys. Rev. Lett.* **100**, 246601 (2008).

⁷N. Roch, S. Florens, V. Bouchiat, W. Wernsdorfer, and F. Balestro, “Quantum phase transition in a single-molecule quantum dot,” *Nature* **453** (2008).

⁸Z. Iftikhar, A. Anthore, A. K. Mitchell, F. D. Parmentier, U. Gennser, A. Ouerghi, A. Cavanna, C. Mora, P. Simon, and F. Pierre, “Tunable quantum criticality and super-ballistic transport in a “charge” kondo circuit,” *Science* **360**, 1315–1320 (2018), <http://science.sciencemag.org/content/360/6395/1315.full.pdf>.

⁹G. Cohen and E. Rabani, “Memory effects in nonequilibrium quantum impurity models,” *Phys. Rev. B* **84**, 075150 (2011).

¹⁰E. Gull, A. J. Millis, A. I. Lichtenstein, A. N. Rubtsov, M. Troyer, and P. Werner, “Continuous-time monte carlo methods for quantum impurity models,” *Rev. Mod. Phys.* **83**, 349–404 (2011).

¹¹L. Mühlbacher and E. Rabani, “Real-time path integral approach to nonequilibrium many-body quantum systems,” *Phys. Rev. Lett.* **100**, 176403 (2008).

¹²M. Schiró and M. Fabrizio, “Real-time diagrammatic monte carlo for nonequilibrium quantum transport,” *Phys. Rev. B* **79**, 153302 (2009).

¹³P. Werner, T. Oka, and A. J. Millis, “Diagrammatic monte carlo simulation of nonequilibrium systems,” *Phys. Rev. B* **79**, 035320 (2009).

¹⁴G. Cohen, E. Gull, D. R. Reichman, A. J. Millis, and E. Rabani, “Numerically exact long-time magnetization dynamics at the nonequilibrium kondo crossover of the anderson impurity model,” *Phys. Rev. B* **87**, 195108 (2013).

¹⁵R. E. V. Profumo, C. Groth, L. Messio, O. Parcollet, and X. Waintal, “Quantum monte carlo for correlated out-of-equilibrium nanoelectronic devices,” *Phys. Rev. B* **91**, 245154 (2015).

¹⁶G. Cohen, E. Gull, D. R. Reichman, and A. J. Millis, “Taming the dynamical sign problem in real-time evolution of quantum many-body problems,” *Phys. Rev. Lett.* **115**, 266802 (2015).

¹⁷H.-T. Chen, G. Cohen, and D. R. Reichman, “Inchworm monte carlo for exact non-adiabatic dynamics. i. theory and algorithms,” *The Journal of Chemical Physics* **146**, 054105 (2017), <https://doi.org/10.1063/1.4974328>.

¹⁸H.-T. Chen, G. Cohen, and D. R. Reichman, “Inchworm monte carlo for exact non-adiabatic dynamics. ii. benchmarks and comparison with established methods,” *The Journal of Chemical Physics* **146**, 054106 (2017), <https://doi.org/10.1063/1.4974329>.

¹⁹I. Bloch, J. Dalibard, and S. Nascimbène, “Quantum simulations with ultracold quantum gases,” *Nature Physics* **8**, 267 EP – (2012).

²⁰R. Blatt and C. F. Roos, “Quantum simulations with trapped ions,” *Nature Physics* **8**, 277 EP – (2012).

²¹A. A. Houck, H. E. Tureci, and J. Koch, “On-chip quantum simulation with superconducting circuits,” *Nature Physics* **8** (2012).

²²K. L. Hur, L. Henriët, A. Petrescu, K. Plekhanov, G. Roux, and M. Schiró, “Many-body quantum electrodynamics networks: Non-equilibrium condensed matter physics with light,” *Comptes Rendus Physique* **17**, 808 – 835 (2016), polariton physics / Physique des polaritons.

²³H.-P. Breuer and F. Petruccione, *The theory of open quantum systems*, 1st ed. (Oxford University Press, USA, 2002).

²⁴S. Diehl, A. Micheli, A. Kantian, B. Kraus, H. P. Büchler, and P. Zoller, “Quantum states and phases in driven open quantum systems with cold atoms,” *Nat Phys* **4**, 878–883 (2008).

²⁵F. Verstraete, M. M. Wolf, and J. Ignacio Cirac, “Quantum computation and quantum-state engineering driven by dissipation,”

- Nat Phys **5**, 633–636 (2009).
- ²⁶K. W. Murch, U. Vool, D. Zhou, S. J. Weber, S. M. Girvin, and I. Siddiqi, “Cavity-assisted quantum bath engineering,” Phys. Rev. Lett. **109**, 183602 (2012).
 - ²⁷M. R. Delbecq, V. Schmitt, F. D. Parmentier, N. Roch, J. J. Viennot, G. Fève, B. Huard, C. Mora, A. Cottet, and T. Kontos, “Coupling a quantum dot, fermionic leads, and a microwave cavity on a chip,” Phys. Rev. Lett. **107**, 256804 (2011).
 - ²⁸M. Schiró and K. Le Hur, “Tunable hybrid quantum electrodynamics from nonlinear electron transport,” Phys. Rev. B **89**, 195127 (2014).
 - ²⁹L. E. Bruhat, J. J. Viennot, M. C. Dartailh, M. M. Desjardins, T. Kontos, and A. Cottet, “Cavity photons as a probe for charge relaxation resistance and photon emission in a quantum dot coupled to normal and superconducting continua,” Phys. Rev. X **6**, 021014 (2016).
 - ³⁰A. Cottet, M. C. Dartailh, M. M. Desjardins, T. Cubaynes, L. C. Contamin, M. Delbecq, J. J. Viennot, L. E. Bruhat, B. Douçot, and T. Kontos, “Cavity qed with hybrid nanocircuits: from atomic-like physics to condensed matter phenomena,” Journal of Physics: Condensed Matter **29**, 433002 (2017).
 - ³¹B.-H. Liu, L. Li, Y.-F. Huang, C.-F. Li, G.-C. Guo, E.-M. Laine, H.-P. Breuer, and J. Piilo, “Experimental control of the transition from markovian to non-markovian dynamics of open quantum systems,” Nat Phys **7**, 931–934 (2011).
 - ³²Ángel Rivas, S. F. Huelga, and M. B. Plenio, “Quantum non-markovianity: characterization, quantification and detection,” Reports on Progress in Physics **77**, 094001 (2014).
 - ³³H.-P. Breuer, E.-M. Laine, J. Piilo, and B. Vacchini, “*Colloquium* : Non-markovian dynamics in open quantum systems,” Rev. Mod. Phys. **88**, 021002 (2016).
 - ³⁴H. Breuer and F. Petruccione, *The Theory of Open Quantum Systems* (OUP Oxford, 2007).
 - ³⁵M. Schiró and M. Fabrizio, “Real-time diagrammatic monte carlo for nonequilibrium quantum transport,” Physical Review B **79**, 153302 (2009).
 - ³⁶H. Aoki, N. Tsuji, M. Eckstein, M. Kollar, T. Oka, and P. Werner, “Nonequilibrium dynamical mean-field theory and its applications,” Rev. Mod. Phys. **86**, 779–837 (2014).
 - ³⁷A. Rüegg, E. Gull, G. A. Fiete, and A. J. Millis, “Sum rule violation in self-consistent hybridization expansions,” Phys. Rev. B **87**, 075124 (2013).
 - ³⁸H. Carmichael, *Statistical Methods in Quantum Optics 1: Master Equations and Fokker-Planck Equations*, Physics and Astronomy Online Library (Springer, 1999).
 - ³⁹J. Schwinger, “Brownian motion of a quantum oscillator,” Journal of Mathematical Physics **2**, 407–432 (1961), <https://doi.org/10.1063/1.1703727>.
 - ⁴⁰L. V. Keldysh, “Diagram technique for nonequilibrium processes,” Zh. Eksp. Teor. Fiz. **47**, 1018 (1964).
 - ⁴¹P. Danielewicz, “Quantum theory of nonequilibrium processes ii. application to nuclear collisions,” Annals of Physics **152**, 305 – 326 (1984).
 - ⁴²P. Danielewicz, “Quantum theory of nonequilibrium processes, i,” Annals of Physics **152**, 239 – 304 (1984).
 - ⁴³M. Wagner, “Expansions of nonequilibrium green’s functions,” Phys. Rev. B **44**, 6104–6117 (1991).
 - ⁴⁴M. Schiró, “Real-time dynamics in quantum impurity models with diagrammatic monte carlo,” Phys. Rev. B **81**, 085126 (2010).
 - ⁴⁵C. W. Gardiner and M. J. Collett, “Input and output in damped quantum systems: Quantum stochastic differential equations and the master equation,” Phys. Rev. A **31**, 3761–3774 (1985).
 - ⁴⁶P. Werner, A. Comanac, L. de’ Medici, M. Troyer, and A. J. Millis, “Continuous-time solver for quantum impurity models,” Phys. Rev. Lett. **97**, 076405 (2006).
 - ⁴⁷H. U. R. Strand, M. Eckstein, and P. Werner, “Nonequilibrium dynamical mean-field theory for bosonic lattice models,” Phys. Rev. X **5**, 011038 (2015).
 - ⁴⁸F. Peronaci, M. Schiró, and O. Parcollet, “Resonant thermalization of periodically driven strongly correlated electrons,” Phys. Rev. Lett. **120**, 197601 (2018).